Centroiding Caused Errors in Tracking and Adaptive Optics

J.J. Garretson
United States Space Force, Schriever SFB, CO 80912

ABSTRACT

Strong correlation between the estimated tilt given by centroiding, sometimes referred to as the centroid tilt, and the gradient tilt (G-tilt) decreases under certain conditions. It can be demonstrated in some scenarios that there is higher correlation between the centroid estimated tilt and Zernike tilt (Z-tilt). This is true specifically when a threshold is applied, or in the presence of strong fluctuations of atmosphere. When an extended target or beam is being tracked there may also be lower tilt-centroid correlation over all, but this error may also have less dependency on phase fluctuation strength. Simulations have been performed to show various dependencies of tilt-centroid correlation and tilt-centroid residual error, also known as centroid anisoplanatism. Correlation between centroid anisoplanatism and Zernike coma, as well as the effects of thresholding are discussed. Correlation between G-tilt, a combined tilt-coma function, and various centroid types are also explored. There is a need to better understand centroids and their effects in both tracking and adaptive optics technology. Developing this understanding will lead to improved jitter mitigation techniques, wavefront estimation, and less resident space object state covariance.

1. INTRODUCTION

Image centroiding is done routinely in many optical technologies and space situational awareness techniques. Devices such as Shack-Hartmann wavefront sensors and position sensitive devices use centroids to estimate wavefront tilts. Centroids have a long history of being used in resident space object tracking, specifically for geostationary objects, and satellite state estimation. In lay terms, the centroided image is used to estimate an angle. This angle could be wavefront tilt, or it may be the angle off boresight or optical mechanical axis. It's observed that the value of the estimated tilt from centroiding varies from that of the actual tilt. This residual error, termed centroid anisoplanatism, changes strength under varying conditions and is stochastic. During most scenarios centroid anisoplanatism can be ignored because it is quite minor compared to other sources of error such as jitter or higher order aberrations. In moderate to strong atmospheric fluctuations centroid anisoplanatism can be significant, inducing Strehl ratios as low as 0.5 [1]. It is possible that this is a primary source of performance degradation for traditional Shack-Hartmann wavefront sensors as phase fluctuations grow stronger. Centroid anisoplanatism strength is also impacted by source and receiver characteristics.

Tilt is traditionally defined as either the least squares fit of the phase over an aperture, also known as Zernike tilt or Z-tilt. The other definition of tilt is the is the gradient of the phase over an aperture, also known as gradient tilt or G-tilt. Centroid anisoplanatism was first defined by Tavis and Yura as the error between the estimated tilt from a centroid and Z-tilt [2]. Others have adapted the definition to mean the error between centroid estimated tilt and G-tilt. Previous efforts to understand centroid anisoplanatism have been limited to certain scenarios. There are no general analytical expressions for the autocovariance of centroid anisoplanatism. The complication in developing a general expression is in solving for the autocovariance of the centroid position and the covariance between the centroid estimated tilt and the Z or G-tilt [3] [4]. When doing so it becomes apparent that the fourth order moment of the optical field must be known. The fourth order moment of the optical field can only be approximated and is limited to expressions for specific scenarios. It becomes even more convoluted when a centroid is performed on thresholded or weighted imagery.

Centroid anisoplanatism is well understood when centroiding a point source through weak fluctuations [2]. Certain approximations can be made for point sources in weak fluctuations, such as the Rytov approximation [5]. It was also shown by Tavis and Yura that when centroiding in weak fluctuations G-tilt can approximate centroid estimated tilt [2][6]. There was then follow-on work to show that the centroid anisoplanatism has strong correlation to Zernike coma [1]. Scintillation was then shown to not be a factor, but only in weak fluctuations [7]. There have also been simulations showing that in strong fluctuations scintillation does contribute to centroid anisoplanatism [9]. Centroid and centroid anisoplanatism autocovariance can be expressed when it is assumed that the optical field is circular complex Gaussian [3][8]. Most recently it has been shown that phase discontinuities, known as branch cuts and

branch points, may also produce centroid anisoplanatism [10]. Implications of thresholding and other alterations to the image prior to finding the centroid are less understood. Previous efforts have also not fully explored the effects of coma and its relationship to centroid anisoplanatism in moderate to strong fluctuations.

2. BACKGROUND

2.1. Tilt and Centroids

All tilts defined are in units of radians, but they could also be defined in arcseconds depending on the normalization. As previously discussed, Z-tilt is the least squares fit of the optical phase over an aperture as seen by Eq 2.1 [11].

$$\vec{\theta}_Z = \frac{1}{\kappa}\vec{\alpha}_{2-3} = \frac{1}{\kappa\pi R^4}\iint W(u,v)\; 2R\vec{\rho}\;\Theta(Ru,Rv)\; dudv \qquad \text{(Eq. 2.1)}$$

Value $\vec{\rho}$ is a unit vector $[u \quad v]^T$, $\Theta(Ru,Rv)$ is the phase of the optical field over the aperture, R is the radius of the aperture with diameter D, κ is the angular wavenumber, and the function $W(u,v)$ is a unit circle. Gradient tilt is the average gradient of the optical field phase at the aperture [2] and is defined as:

$$\vec{\theta}_G = \frac{1}{\kappa}\vec{\alpha}_G = \frac{1}{\kappa\pi R^2}\iint W(u,v)\;\nabla[\Theta(Ru,Rv)]\; dudv \qquad \text{(Eq. 2.2)}$$

where ∇ is the gradient operator. The centroid expression is used in many fields and is commonly referred to as the center of gravity equation. In this case it is the center of the image intensity $I(x,y)$. The centroid being in the focal plane has position vector $\vec{r} = [x \quad y]^T$. The standard centroid equation [3] is:

$$\overrightarrow{\Delta r_C} = \frac{1}{I_0}\iint \vec{r}\, I(x,y)\; dxdy \qquad \text{(Eq. 2.3)}$$

Value I_0 is the expected total image intensity. When thresholding or weighting an image before finding the centroid one must use the altered centroid equation. Thresholding is most often performed to omit the noise floor from the image, but also omits parts of the image intensity that falls below the noise floor. The altered centroid equation [12] can be defined as:

$$\overrightarrow{\Delta r_A} = \frac{1}{A_0}\iint \vec{r}\left[\widetilde{H}(I-T)\, M(x,y)\, I(x,y) - cT\widetilde{H}(I-T)\right] dxdy \qquad \text{(Eq. 2.4)}$$

$M(x,y)$ is a weighting function, A_0 is the expected altered total image intensity, and T is the threshold value which is between 0 and 1. Value c sets the altered centroid type and is either 0 for a type 1 centroid or 1 for a type 2 centroid. Function $\widetilde{H}(I-T)$ is a heavy side function that implements the threshold and is defined as:

$$\widetilde{H}(I-T)\begin{cases} 0 & I-T<0 \\ 1 & I-T\geq 0 \end{cases} \qquad \text{(Eq. 2.5)}$$

When converting the spatial value produced from centroiding to an angle the focal length is used as the adjacent length since the desired tilt is in the pupil plane. Estimated centroid tilt is thus:

$$\overrightarrow{\theta_C} = tan\left(\overrightarrow{\Delta r_C}/f\right) \qquad \text{(Eq. 2.6)}$$

Coma has been shown to be a large contributor to centroid anisoplanatism [1]. Coma aberrations lead to the image intensity to spread or smear more in one direction than another. In theory the overall center of the image intensity does not change in ideal diffraction-limited, noise free systems. Zernike coma coefficient as defined by Noll [11] is:

$$\vec{\alpha}_{7-8} = \frac{1}{\pi R^2(9R^4-16R^2+8)}\iint W(u,v)\sqrt{8}R\vec{\rho}(R^2 3(u^2+v^2)-2)\;\Theta(Ru,Rv)\; dudv \qquad \text{(Eq. 2.7)}$$

It has been understood that the estimated tilt from centroiding and the actual tilt are well correlated, yet not equivalent. Fig. 1 shows a phase center cut of tilts and centroid estimated tilts for both an applied Zernike tilt (left) and an applied coma (right). Fig 1 is using a point source as the source of the optical field. Fig. 2 shows the same as

Fig. 1, but a top-hat beam was the source of the optical field. The top-hat beam had a width a third of the aperture diameter.

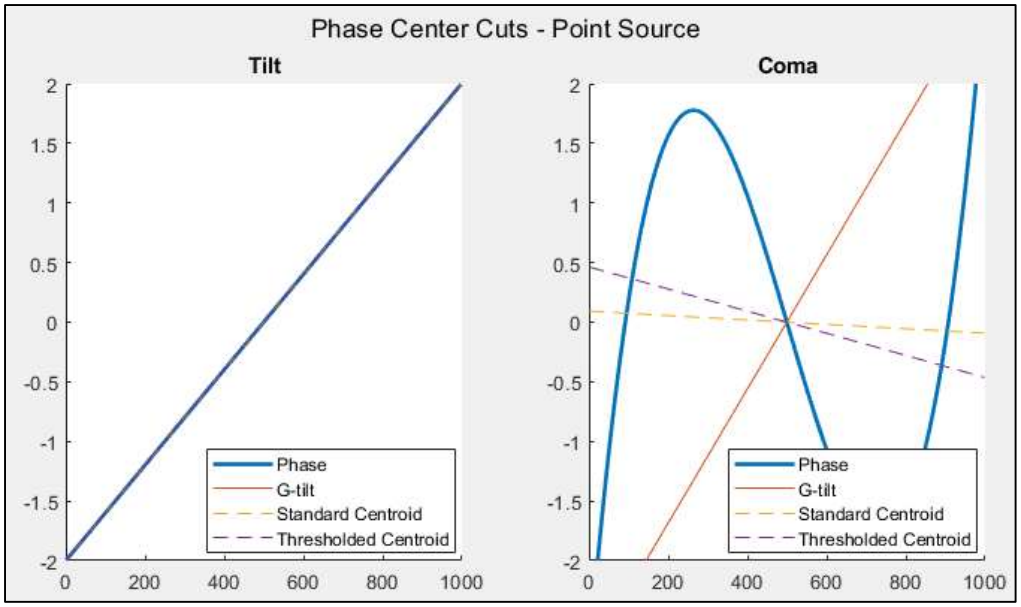

Fig. 1. Estimated and Actual Tilts from a Point Source

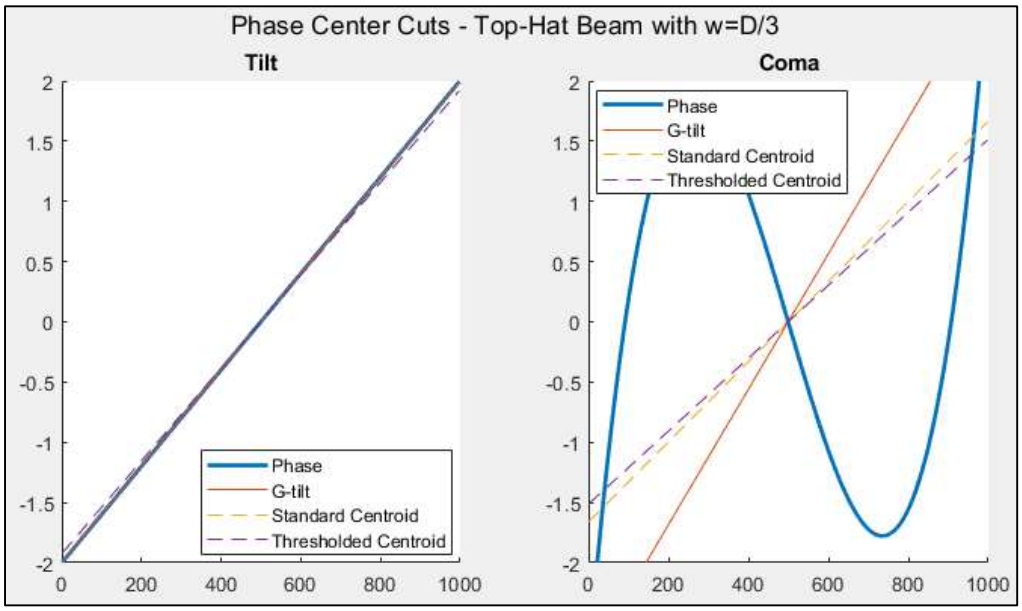

Fig. 2. Estimated and Actual Tilts from a Top-hat Beam

These figures show that centroid estimated tilts perform differently based on the source of the optical field. Centroid anisoplanatism has more than just a dependency on coma strength. Centroid estimated tilts are functions of image intensity which leads that they also will share similar dependencies to that image intensity.

2.2. Phase Fluctuation Strength

Fluctuations of the index of refraction of the atmosphere directly cause fluctuations in the optical field. These fluctuations may be split into fluctuations in intensity, also known as scintillation, and fluctuations of phase. When discussing the strength of these fluctuations several values are commonly used. Rytov variance is one such value and is specifically used to describe the fluctuation strength of Kolmogorov atmosphere. It also can be made specific

to plane or spherical waves, and can also be modified for gaussian beams [5]. Eq 2.8 is the Rytov variance for a plane wave. When Rytov variance is near unity the fluctuations are said to be moderate, less than unity weak, and greater than unity strong.

$$\sigma_1^2 = 1.23 C_n^2 \kappa^{7/6} L^{11/6} \quad \text{(Eq. 2.8)}$$

Value C_n^2 is the refractive-index structure parameter and L is the path length from source to the receiving aperture. The ratio of the aperture size to the atmospheric coherence diameter is another such value to describe atmospheric turbulence strength. Atmospheric coherence diameter, also known as Fried's parameter or the seeing parameter, describes the diameter of an ideal system that images at the same angular resolution as a system being impacted by the atmosphere [5][7]. Atmospheric coherence length for a plane wave is defined as:

$$r_0 = (0.42 \kappa^2 C_n^2 L)^{-3/5} \quad \text{(Eq. 2.9)}$$

Eq. 2.9 can also be defined with a constant of 0.16 for both spherical waves and collimated beams instead of 0.42 which is for plane waves. It can also be modified with a $sec(\zeta)$ for different look angles from zenith.

Power spectral density, or PSD, of phase fluctuations will be used when determining covariances of tilts and coma. Kolmogorov turbulence [11][5] will be assumed and the Kolmogorov PSD for phase fluctuations is:

$$\Phi_K(f) = 0.0022896 r_0^{-5/3} (f)^{-11/3} \quad \text{(Eq. 2.10)}$$

It is important to note that the atmosphere is only one source of tilt. Other sources of tilt are aero-optical turbulence and mechanical vibrations [13]. This is especially true if the receiver is on board a moving ground vehicle, aircraft, or spacecraft. Laser speckle may also induce a tilt if a coherent illuminator is being used [4]. These sources of tilt will not be the focus of this paper.

3. METHODOLOGY

Contributions that coma have on estimated and G tilt will be explored. Coma will first be proportionally added to Z-tilt to produce the function:

$$\alpha_{CX,CY} = \alpha_{2,3} + \gamma \alpha_{8,7} \quad \text{(Eq. 3.1)}$$

Horizontal coma, polynomial 8 in Noll's index, is added to horizontal tilt, 2 in Noll's index. The same is done with the vertical coma and tilt. Scalar γ is a gain on the coma coefficient and will be variable to optimize the correlation per centroid or tilt type. Eq. 3.2 is the covariance function for Zernike polynomial coefficients [11][15][16].

$$\left\langle \alpha_j \alpha_{j'}^* \right\rangle = R^{-2} \int_0^{2\pi} \int_0^{\infty} Q_j(f,\phi) Q_{j'}(f,\phi) \Phi_K(f/R) df d\phi \quad \text{(Eq. 3.2)}$$

Brackets ⟨ ⟩ represent the ensemble expected value operator. Function $Q_j(f,\phi)$ is a PSD filter function as defined by Noll [11][16] and is the Fourier transform of j-th Zernike polynomial. Filter functions for Z-tilt and coma are Eqs. 3.3-3.6. The gradient operator also produces a filter function [17][18] when Fourier transformed which is Eq 3.7 and Eq. 3.8.

$$Q_2 = 2i \frac{J_2(2\pi f)}{\pi f} \cos(\phi) \quad \text{(Eq. 3.3)} \qquad Q_3 = 2i \frac{J_2(2\pi f)}{\pi f} \sin(\phi) \quad \text{(Eq. 3.4)}$$

$$Q_8 = -2\sqrt{2}\, i \frac{J_4(2\pi f)}{\pi f} \cos(\phi) \quad \text{(Eq. 3.5)} \qquad Q_7 = -2\sqrt{2}\, i \frac{J_4(2\pi f)}{\pi f} \sin(\phi) \quad \text{(Eq. 3.6)}$$

$$Q_{GX} = -2\, i \frac{J_1(2\pi f)}{f} \cos(\phi) \quad \text{(Eq. 3.7)} \qquad Q_{GY} = -2\, i \frac{J_1(2\pi f)}{f} \sin(\phi) \quad \text{(Eq. 3.8)}$$

$$\int_0^{\infty} t^{-p} J_\mu(at) J_\nu(at) dt = \frac{(0.5a)^{p-1} \Gamma\left(0.5(\mu+\nu-p+1)\right) \Gamma(p)}{2\, \Gamma\left(0.5(\nu-\mu+p+1)\right) \Gamma\left(0.5(\mu-\nu+p+1)\right) \Gamma\left(0.5(\mu+\nu+p+1)\right)} \quad \text{(Eq. 3.9)}$$

Function $J_n(t)$ is a Bessel function of the first kind and n-th order. These filter functions have been defined in polar frequency coordinates for simplicity. Eq. 3.9 is an identity of Bessel functions and can be found in many Bessel function identity manuals [19]. Following Noll's work and using Eq. 3.9 the normalized covariances of Zernike polynomial coefficients 2 through 8 are found specifically for a Kolmogorov atmosphere and are presented in Table 1. These are normalized by the value of $(D/r_0)^{5/3}$.

Table 1. Normalized Zernike Coefficient Covariances

Noll Index	2 "X-tilt"	3 "Y-tilt"	4 "Focus"	5 "Ob. Astig."	6 "V. Astig."	7 "V. Coma"	8 "H. Coma"
2 "H. Tilt"	0.4489	0	0	0	0	0	0.0142
3 "V. Tilt"	0	0.4489	0	0	0	0.0142	0
4 "Focus"	0	0	0.0232	0	0	0	0
5 "Ob. Astig."	0	0	0	0.0232	0	0	0
6 "V. Astig."	0	0	0	0	0.0232	0	0
7 "V. Coma"	0	0.0142	0	0	0	0.00619	0
8 "H. Coma"	0.0142	0	0	0	0	0	0.00619

Normalized variance of G-tilt in Kolmogorov atmosphere is 0.4190, the covariance between Z-tilt and G-tilt is 0.4302, and the covariance between coma and G-tilt is 0.00778. When solving for both the variance of Eq. 3.1 the following is produced:

$$\langle \alpha_{CX,CY}^2 \rangle = \langle \alpha_{2,3}^2 \rangle + \gamma^2 \langle \alpha_{8,7}^2 \rangle + 2\gamma \langle \alpha_{2,3}\alpha_{8,7} \rangle \quad \text{(Eq. 3.10)}$$

The covariance between the tilt-coma function and the Z-tilt, or G-tilt, are Eq 3.11 and 3.12 respectively.

$$\langle \alpha_{2,3}\alpha_{CX,CY} \rangle = \langle \alpha_{2,3}^2 \rangle + \gamma \langle \alpha_{2,3}\alpha_{8,7} \rangle \quad \text{(Eq. 3.11)}$$

$$\langle \alpha_{GX,GY}\alpha_{CX,CY} \rangle = \langle \alpha_{GX,GY}\alpha_{2,3} \rangle + \gamma \langle \alpha_{GX,GY}\alpha_{8,7} \rangle \quad \text{(Eq. 3.12)}$$

These equations reduce to the following using the Kolmogorov PSD for phase fluctuations:

$$\langle \alpha_{CX,CY}^2 \rangle = (0.00619\gamma^2 + 0.0283\gamma + 0.4489)\left({}^{D}/_{r_0}\right)^{\frac{5}{3}} \quad \text{(Eq. 3.13)}$$

$$\langle \alpha_{2,3}\alpha_{CX,CY} \rangle = (0.0142\gamma + 0.4489)\left({}^{D}/_{r_0}\right)^{\frac{5}{3}} \quad \text{(Eq. 3.14)}$$

$$\langle \alpha_{GX,GY}\alpha_{CX,CY} \rangle = (0.00778\gamma + 0.4302)\left({}^{D}/_{r_0}\right)^{\frac{5}{3}} \quad \text{(Eq. 3.15)}$$

The correlation coefficient between Z-tilt and the combined tilt-coma function in Kolmogorov atmosphere is thus:

$$corr(\alpha_{2,3}\alpha_{CX,CY}) = \frac{\langle \alpha_{2,3}\alpha_{CX,CY} \rangle}{\sqrt{\langle \alpha_{CX,CY}^2 \rangle \langle \alpha_{2,3}^2 \rangle}} = \frac{(0.0142\gamma \quad .4489)}{\sqrt{(0.00278\gamma^2 + 0.0127\gamma \quad .2015)}} \quad \text{(Eq. 3.16)}$$

This results in a maximum correlation of 1 at $\gamma = 0$. Similarly, the correlation coefficient for G-tilt and the combined tilt-coma function yields:

$$corr(\alpha_{2,3}\alpha_{CX,CY}) = \frac{\langle \alpha_{GX,GY}\alpha_{CX,CY} \rangle}{\sqrt{\langle \alpha_{CX,CY}^2 \rangle \langle \alpha_{GX,GY}^2 \rangle}} = \frac{(0.00778\gamma + 0.4302)}{\sqrt{(0.00259\gamma^2 + 0.0119\gamma \quad .1881)}} \quad \text{(Eq. 3.17)}$$

There is a maximum correlation of nearly 1 resulting when $\gamma = -1.019$. Residual error between the combined tilt-coma function and the Z or G-tilt is defined by Eq. 3.18. Variance of the residual error for G-tilt is Eq. 3.19 which reduces to Eq. 3.20 in Kolmogorov atmosphere.

$$\Delta_{Z,G} = \left(\tilde{\theta}_C - \theta_{Z,G}\right) = \kappa^{-1}\left(\alpha_{2,3} + \gamma\alpha_{8,7} - \alpha_{[2,3],[GX,GY]}\right) \quad \text{(Eq. 3.18)}$$

$$\langle\Delta_G^2\rangle = \kappa^{-2}\left(\gamma^2\langle\alpha_{8,7}^2\rangle - 2\gamma\left(\langle\alpha_{8,7}\alpha_{GX,GY}\rangle - \langle\alpha_{8,7}\alpha_{2,3}\rangle\right) + \left(\langle\alpha_{2,3}^2\rangle + \langle\alpha_{GX,GY}^2\rangle - 2\langle\alpha_{2,3}\alpha_{GX,GY}\rangle\right)\right) \quad \text{(Eq. 3.19)}$$

$$\langle\Delta_G^2\rangle = \kappa^{-2}(0.00619\gamma^2 - 0.0128\gamma + 0.00750)\left(D/r_0\right)^{\frac{5}{3}} \quad \text{(Eq. 3.20)}$$

This produces a minimum error between G-tilt and the tilt-coma function of $(9.1704 \times 10^{-4})\kappa^{-2}(D/r_0)^{5/3}$ when the gain is -1.031.

4. SIMULATIONS

4.1. Single Phase Screen Simulations

Three simulations were established to ascertain a better understanding of centroid anisoplanatism. The first being a simple numerical simulation. A random phase screen was generated using Zernike polynomials that included tilt, astigmatism, trefoil, and coma. All polynomial coefficients had unity variances and were independent. An optical transfer function was generated using the random phase screen. The optical transfer function was then Fourier transformed to create a point spread function. Amplitude of the resulting waveform was used in the various centroiding types.

The second simulation was similar to the first, but the Zernike polynomials coefficients were generated randomly using the coefficient covariance matrix provided by Table 1. Value of $(D/r_0)^{5/3}$ was set to 8, which is close to a moderate turbulence strength. This simulation used a wave optics toolbox to propagate a collimated point source to the phase screen, introduce the screen, and then focus the resulting optical field. This simulation setup is very similar to that described in section 4.2 below, but was for a singular controlled phase screen. This phase screen included only the first 11 Zernike polynomials. Recorded data for both simulations included the variances, covariances, and correlations for G-tilt, Z-tilt, Coma, and three different centroids. The three centroids used were a standard centroid, a type 1 thresholded centroid, and a type 2 thresholded centroid. There were 5000 phase realizations simulated for both singular phase screen simulations.

4.2. Volumetric Kolmogorov Atmosphere Simulation

The final simulation performed was a wave optics simulation using a Fresnel propagator. Fig. 3 shows the arrangement of the simulation. Both a simulated point source and top-hat beam were used as sources. Sources were propagated through the random medium, which were Kolmogorov phase screens evenly spaced 250m apart to simulate a volumetric atmosphere. A receiving aperture is placed 2.5km from the source and focuses the wavefront to a focal plane. Table 2 shows other characteristics of the simulation. Lastly, the top hat beam had a diameter one-third of the receiving aperture.

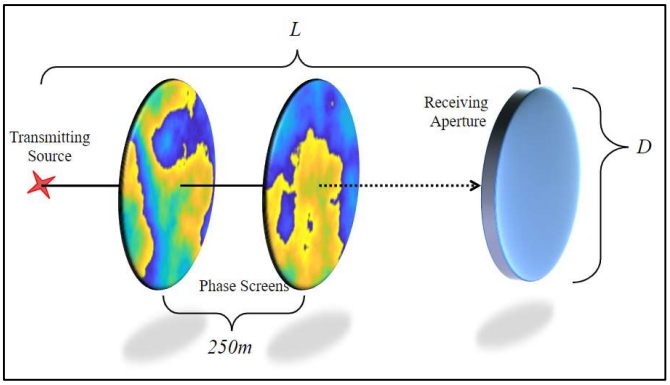

Fig. 3. Wave Optics Simulation Arrangement

Table 2. Wave Optics Simulation Values

Variable	Value
Wavelength (λ)	1μm
Propagation distance (L)	2.5km
Receiving Aperture (D)	0.3m
Grid Size	511
Grid Sample Size	0.002m
Realizations	500
Samples of C_n^2	50 evenly spaced between $10^{-16.5}$ and 10^{-13}
Centroid threshold (T)	0.1, 0.01, and 0.001

5. RESULTS

5.1. Centroid Anisoplanatism Analysis for Unity Variance Zernike-Polynomials

Fig. 4 plots a small portion the generated Z-tilt coefficient, the calculated G-tilt, and the centroids from the unity variance simulation. Variances, covariances, and correlations from the combined vertical and horizontal realizations are provided in Table 3.

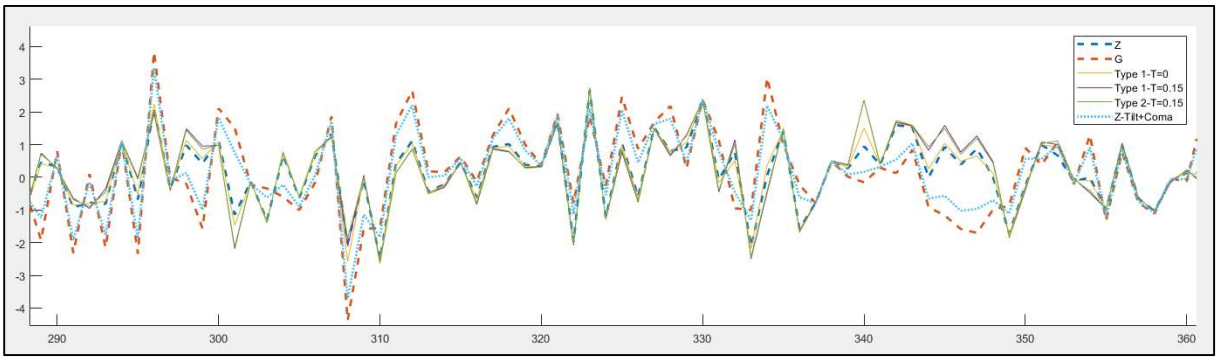

Fig. 4. Realizations from the Unity Variance Single Phase Screen Simulation

Table 3. Variance and Correlation Results (Unity Variance)

Variable	Result	Variable	Result	Variable	Result
$\langle\alpha_{2,3}^2\rangle$	1	$corr(\alpha_{2,3}r_C)$	0.92	$corr(\alpha_{GX,GY}r_C)$	0.36
$\langle\alpha_{GX,GY}^2\rangle$	2.94	$corr(\alpha_{2,3}r_{A1})$	0.71	$corr(\alpha_{GX,GY}r_{A1})$	-0.08
$\langle\alpha_{8,7}^2\rangle$	1	$corr(\alpha_{2,3}r_{A2})$	0.66	$corr(\alpha_{GX,GY}r_{A2})$	-0.16
$\langle\alpha_{2,3}\alpha_{8,7}\rangle$	0	$\langle r_C^2\rangle$	1.2		
$\langle\alpha_{GX,GY}\alpha_{8,7}\rangle$	1.39	$\langle r_{A1}^2\rangle$	2.1		
$\langle\alpha_{2,3}\alpha_{GX,GY}\rangle$	0.99	$\langle r_{A2}^2\rangle$	2.35		

It is observed that when the variance of coma is just as high as Z-tilt that the centroids are more closely correlated to Z-tilt than they are to G-tilt. It should also be noted that the correlation between G-tilt and coma is strong, calculated to be 0.81 from Table 3 results. Variance of the combined tilt-coma function as the gain value, γ, is adjusted between -4 and 4 is provided by Fig. 5. Correlations between the combined tilt-coma function and the centroids are displayed in Fig. 6. It can be observed in Fig. 6 that the optimum gains for Eq 3.1 are the maximum correlations. Fig. 7 is the RMS error between the combined tilt-coma function and the centroids, to include G-tilt. The combined function is equivalent to Z-tilt when the gain is zero, and equivalent to G-tilt when the RMS error is zero and the correlation is one. The combined tilt-coma function is equal to G-tilt at $\gamma = 1.4$ for this specific scenario of unity variance of the Zernike polynomial coefficients.

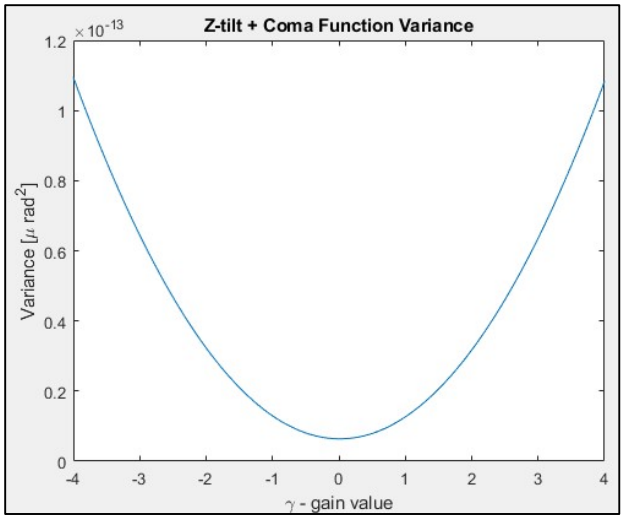

Fig. 5. Variance of the Tilt- Coma Function, Unity Variance

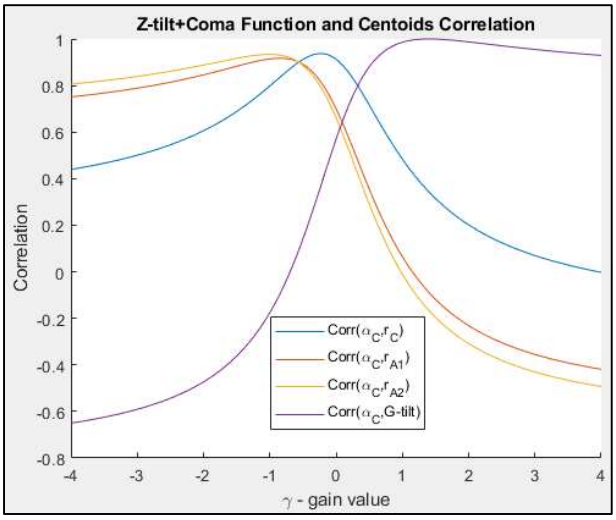

Fig. 6. Correlation of Tilt-Coma Function, Centroids/ G-tilt, Unity Variance

Table 4. Centroid Anisoplanatism Correlation to Coma (Unity Variance)

Centroid Type	G-tilt C.A.-Coma Correlation	Z-tilt C.A.-Coma Correlation
Standard	0.97	0.52
Type 1 with 0.15 threshold	0.97	0.83
Type 2 with 0.15 threshold	0.98	0.88

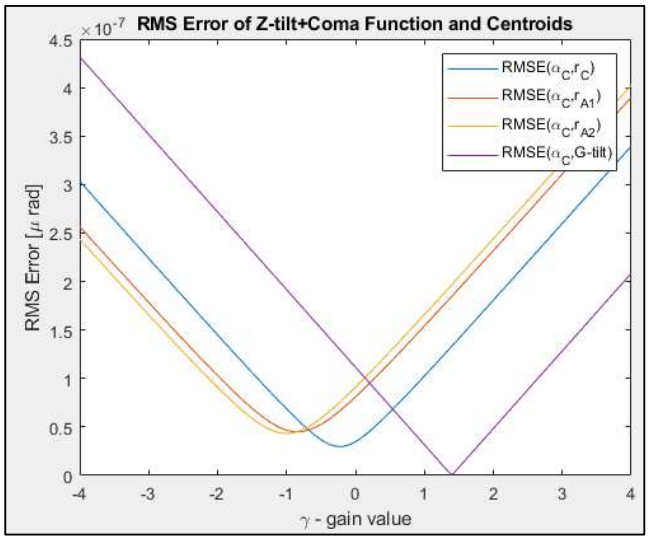

Fig. 7. RMS Error Between Tilt-Coma Function and Centroids/ G-tilt, Unity Variance

Table 4 shows the correlation between the centroid anisoplanatism and coma. These centroid anisoplanatism-coma correlation results, along with the RMS error results, collaborate that with high coma variance relative to the Z-tilt variance centroid anisoplanatism is lower when using Z-tilt. It also confirms that coma is correlated to centroid anisoplanatism for either tilt, but is nearly perfectly correlated to G-tilt centroid anisoplanatism. In this scenario coma was also an additive factor for G-tilt, but was inverse for the centroids. While this scenario is fictional, it does shed light on coma's impact on G-tilt over Z-tilt centroid anisoplanatism. As coma becomes for pronounced it will lead to increased centroid anisoplanatism.

5.2. Centroid Anisoplanatism Analysis for Kolmogorov Variance Zernike-Polynomials

Table 5. Normalized Variance and Correlation Results (Kolmogorov)

Variable	Result	Variable	Result	Variable	Result
$\langle \alpha_{2,3}^2 \rangle$	0.44	$corr(\alpha_{2,3} r_C)$	0.98	$corr(\alpha_{GX,GY} r_C)$	1*
$\langle \alpha_{GX,GY}^2 \rangle$	0.44	$corr(\alpha_{2,3} r_{A1})$	0.98	$corr(\alpha_{GX,GY} r_{A1})$	0.98
$\langle \alpha_{8,7}^2 \rangle$	0.0062	$corr(\alpha_{2,3} r_{A2})$	0.98	$corr(\alpha_{GX,GY} r_{A2})$	0.98
$\langle \alpha_{2,3} \alpha_{8,7} \rangle$	0.013	$\langle r_C^2 \rangle$	0.52		
$\langle \alpha_{GX,GY} \alpha_{8,7} \rangle$	0.019	$\langle r_{A1}^2 \rangle$	0.48		
$\langle \alpha_{2,3} \alpha_{GX,GY} \rangle$	0.43	$\langle r_{A2}^2 \rangle$	0.48		

All recorded correlations and variances in Table 5 are near their expected values. Variances and covariances have been normalized with a D/r_0 of 8. The standard centroid is nearly perfectly correlated to G-tilt in Kolmogorov turbulence, even in moderate fluctuations. Correlation between G-tilt and the standard centroid was 0.9976. All other centroid estimated tilts were highly correlated to both Z and G-tilt. It should be noted the standard centroid was very slightly thresholded to remove a floating-point error seen in the result of section 5.3. The threshold value was set to 10^{-12}.

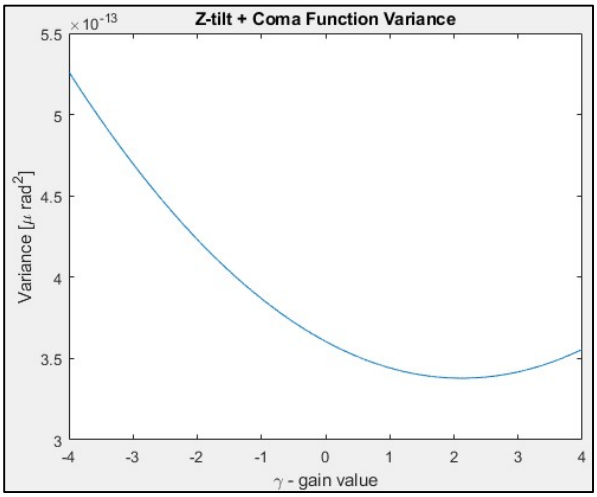

Fig. 8. Variance of the Tilt- Coma Function, Kolmogorov

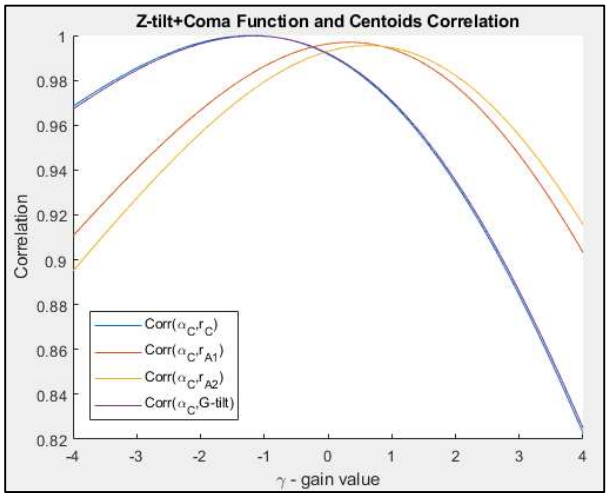

Fig. 9. Correlation of Tilt-Coma Function and Centroids/ G-tilt, Kolmogorov

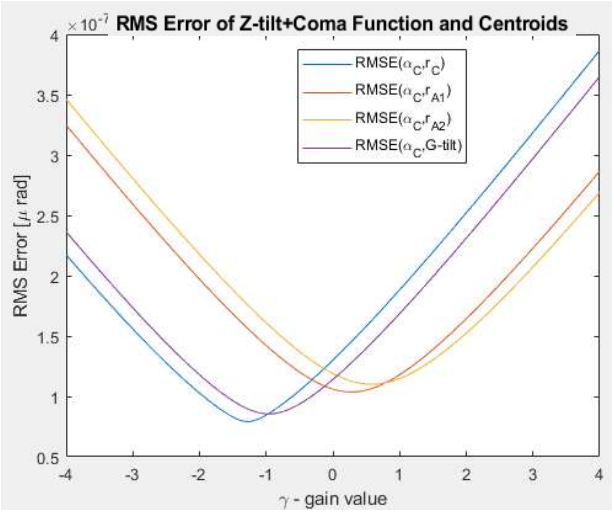

Fig. 10. RMS Error Between Tilt-Coma Function and Centroids/ G-tilt, Kolmogorov

Optimum gain for the tilt-coma function for G-tilt in this scenario is near -1, which was the calculated optimum gain in section 3. The tilt-coma function never is equivalent to G-tilt hence the RMS error never reaching zero. Due to the high degree of correlation between the standard centroid and G-tilt the correlation and RMS error between the tilt-coma function and the standard centroid is nearly the same for G-tilt. Coma has an inverse relationship with G-tilt and the standard centroid, but and additive relationship with the altered centroids. Table 6 shows the correlations between the centroid anisoplanatism and coma. Coma is more correlated to Z-tilt centroid anisoplanatism when a standard centroid is used, but there is less correlation for altered centroids. The opposite is said for G-tilt centroid anisoplanatism. The source of this is due to the low amount of centroid anisoplanatism for G-tilt and a standard centroid, or Z-tilt and altered centroids. When there is a stronger presence of centroid anisoplanatism then coma does have a higher correlation to it.

Table 6. Centroid Anisoplanatism Correlation to Coma (Kolmogorov)

Centroid Type	G-tilt C.A.-Coma Correlation	Z-tilt C.A.-Coma Correlation
Standard	0.41	0.76
Type 1 with 0.15 threshold	0.77	0.28
Type 2 with 0.15 threshold	0.81	0.44

5.3. Analysis of Wave Optics Simulation in Volumetric Kolmogorov Atmosphere

Fig. 11 and 13 show plots of the tilt-centroid correlations as turbulence strength increases for a point source. Fig.11 shows the correlation coefficient for Z-tilt and G-tilt per C_n^2, and Fig. 13 is per D/r_0. Both have vertical lines at unity Rytov variance to denote the transition of weak fluctuations to strong. Fig. 12 and 14 are similar plots to Fig. 11 and 13 but are the results for top-hat beam source.

Results for Z-tilt show that the standard and slightly thresholded centroids have the weakest correlation and the thresholded centroids have the strongest. As the strength in the fluctuations increase the thresholded centroids start to become less correlated to Z-tilt and their rate of decorrelation accelerates in the strong fluctuation regime.

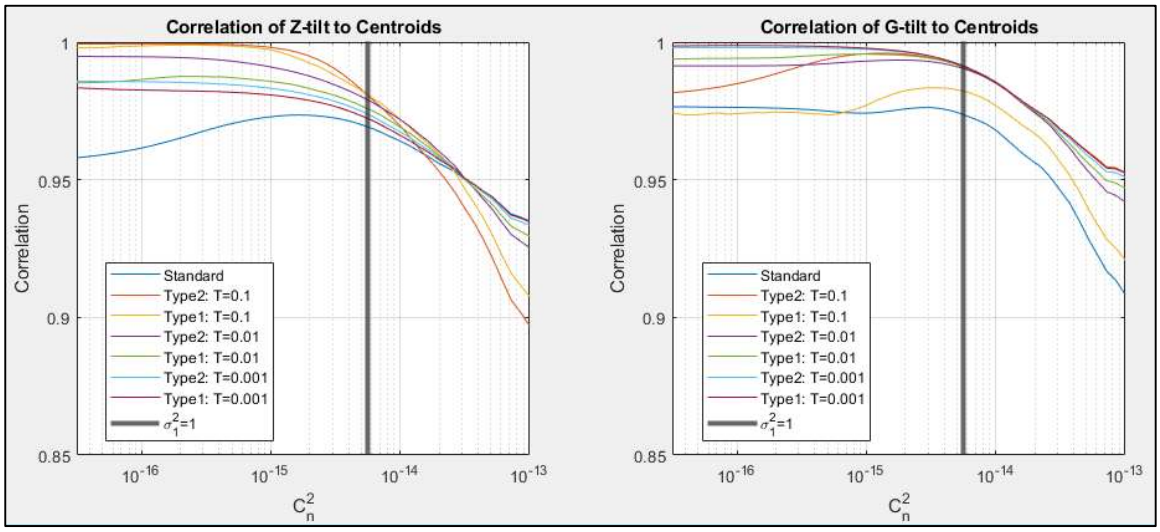

Fig. 11. Tilt-Centroid Correlation per C_n^2 for a Point Source

The top-hat beam source produced correlations overall lower than the point source. Correlations remain flat in weak fluctuations and then start strengthening as the fluctuations enter a moderate regime for Z-tilt. They then peak in the strong regime, but then decrease as fluctuation strength increases. The most correlated centroid to Z-tilt for the top-hat beam source are the standard and slightly thresholded centroids. This is counter to the results for the point source.

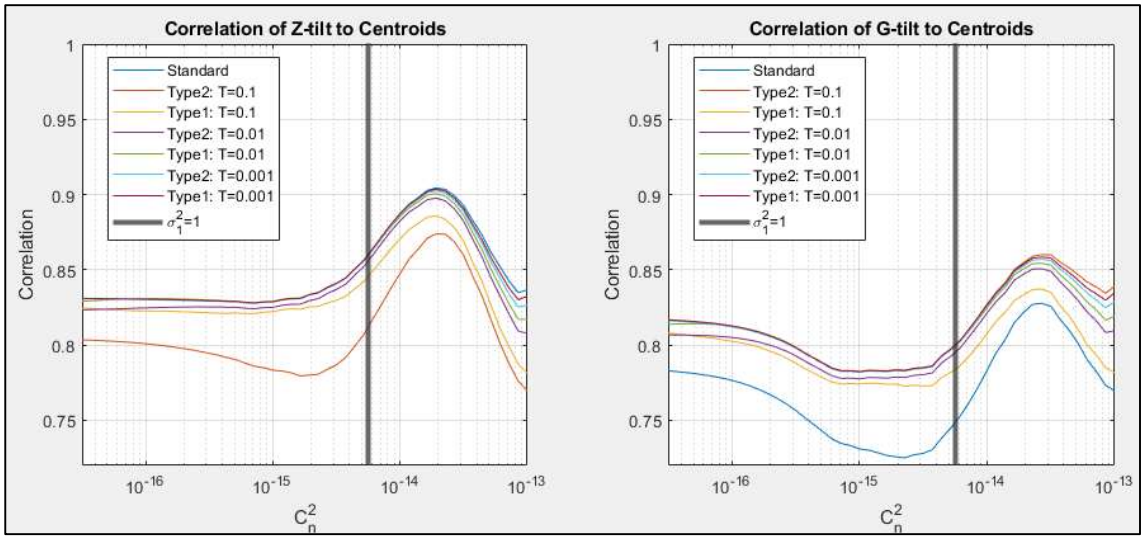

Fig. 12. Tilt-Centroid Correlation per C_n^2 for a Top-Hat Beam

Results for the correlation between centroids and G-tilt are weaker with regards to the standard centroid. The most correlated centroids are slightly thresholded centroids with threshold values of 0.001. This very well could be due to errors in the simulation and the slight threshold corrected for this. This confirms that the standard centroid, or in this case at least a slightly thresholded centroid, has the strongest correlation to G-tilt. Type 2 centroid with a threshold of 0.1 starts with lower correlation, but as fluctuations increase to moderate levels it approaches correlations similar to the slightly thresholded centroids. The Type 1 also increases in correlation in moderate turbulence, but the correlation stays lower relative to all other correlations. Most of the centroids perform similarly until in very strong fluctuations for the G-tilt top-hat beam results. There is a similar pattern to the Z-tilt top-hat beam results of having less correlation in weaker fluctuations and higher correlation in stronger fluctuations.

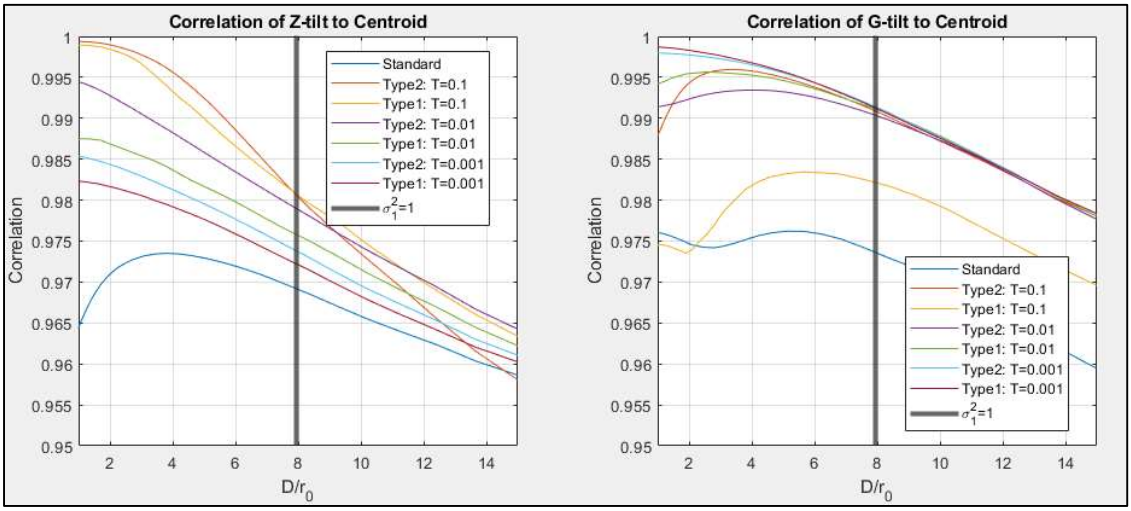

Fig. 13. Tilt-Centroid Correlation per D/r_0 for a Point Source

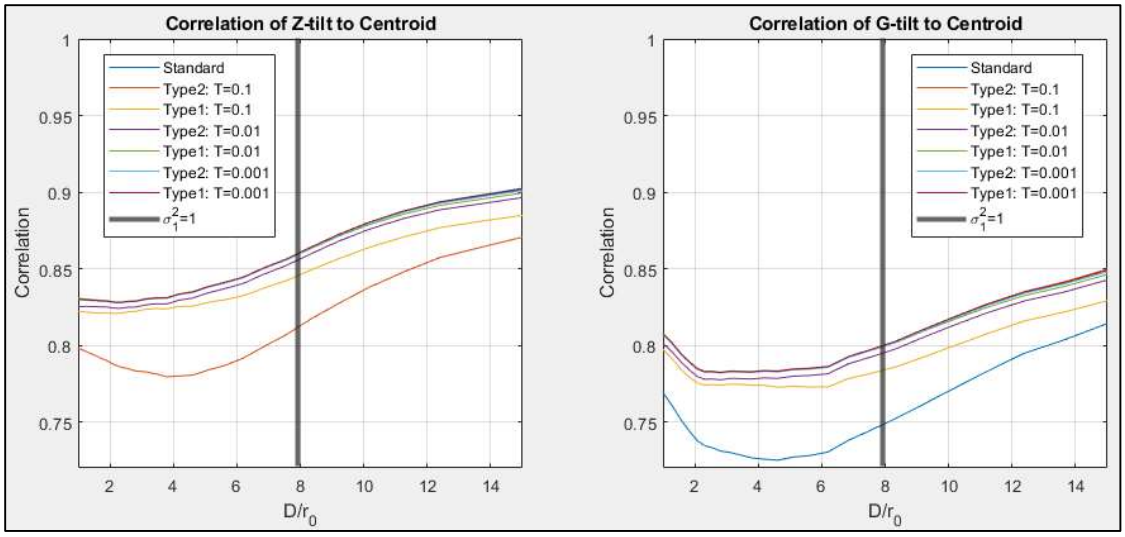

Fig. 14. Tilt-Centroid Correlation per D/r_0 for a Top-Hat Beam

RMS error was also recorded and is plotted in Fig 15. This plot has both the RMS error for G-tilt and Z-tilt. The results for point sources are on the left and the top-hat beam the right. Error for the top-hat beam was higher, over twice as high as the point source results. The lowest RMS error with the point source is the difference between G-tilt and the standard centroid. This is the traditionally expected result. Error between Z-tilt and standard centroid is the lowest for the top hat beam, followed closely by Z-tilt and most other centroid types besides the heavily thresholded ones. Most expected correlations and RMS errors seen in the point source simulation are counter in the top-hat simulation. These results confirm that centroid anisoplanatism has dependencies other than turbulence strength and source characteristics is one of those dependencies.

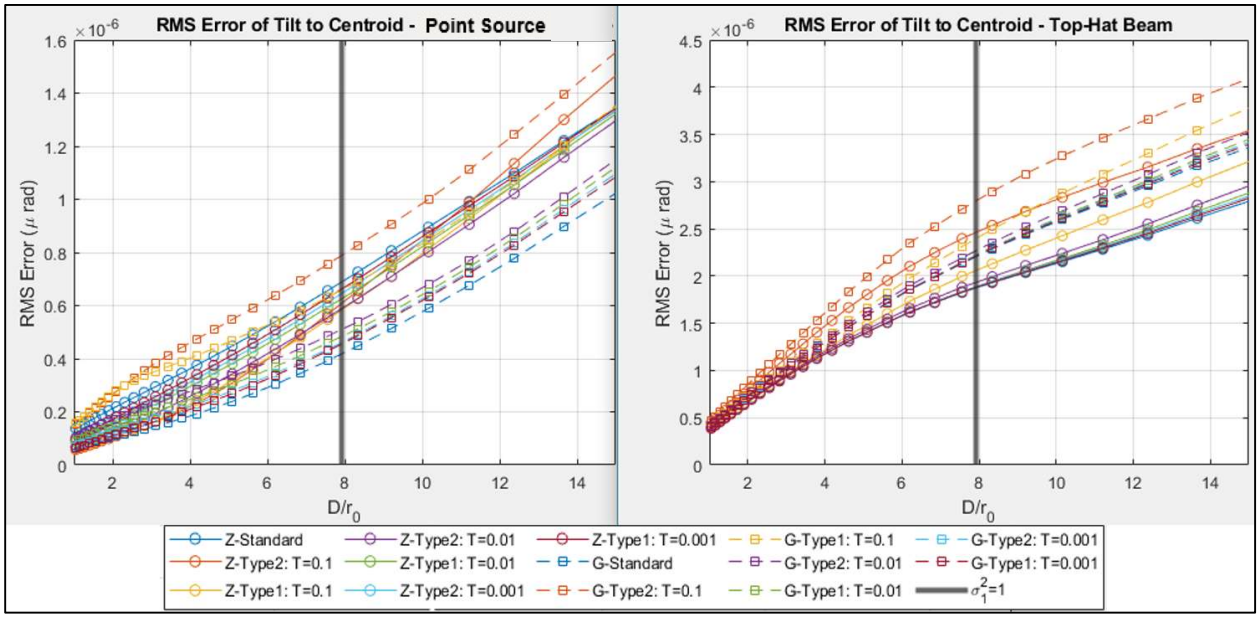

Fig. 15. RMS Error Between Tilts and Centroid Estimates

6. CONCLUSIONS

This paper is meant to bring light to the variability of centroid anisoplanatism and the misconception that G-tilt is always the most closely equivalent to centroid estimated tilts. Results show that when a relatively strong coma to Z-tilt is present that all centroids will be more aligned to Z-tilt. Volumetric wave optics simulations show that in any strength of turbulence that Z-tilt may be more aligned to the standard centroid depending on the source of the optical

field. Moreover, G-tilt is a good approximation of a combined Z-tilt and coma, but it is evident that since coma is not the only variable that impacts centroid anisoplanatism that G-tilt cannot always be the approximation of centroid estimated tilt. Developing a better understanding of centroid anisoplanatism will allow for better adaptive optics, beam control, and tracking techniques. This in turn will reduce the amount of error seen by ground-based imaging systems and in satellite state data.

The views presented are those of the author and do not necessarily represent the views of DoD or its Components.

7. REFERENCES

[1] J. H. Churnside, G. A. Tyler, M. T. Tavis, and H. T. Yura, "Zernike-Polynomial Expansion of Turbulence-Induced Centroid Anisoplanatism," *Opt. Lett.*, vol. 10, no. 6, p. 258, 1985.

[2] H. T. Yura and M. T. Tavis, "Centroid Anisoplanatism," *J. Opt. Soc. Am. A*, vol. 2, no. 5, p. 765, 1985.

[3] D. Burrell, J.J. Garretson, J. Vorenberg, and R. Driggers, "Active vs. passive tracking: when to illuminate?," in *Infrared Imaging Systems: Design, Analysis, Modeling, and Testing XXXIII*, G. C. Holst and D. P. Haefner, Eds., Orlando, United States: SPIE, May 2022, p. 14. doi: 10.1117/12.2619026.

[4] D. J. Burrell, M. F. Spencer, M. K. Beason, and R. G. Driggers, "Active-tracking scaling laws using the noise-equivalent angle due to speckle," *J. Opt. Soc. Am. A*, vol. 40, no. 5, p. 904, May 2023, doi: 10.1364/JOSAA.482777.

[5] L. C. Andrews and R. L. Phillips, *Laser Beam Propagation through Random Media*, 2nd ed. SPIE Press Monograph Vol. PM152, 2005.

[6] M. T. Tavis and H. . Yura, "Strong Turbulence Effects on Short Wavelength Lasers," 1979.

[7] M. T. Tavis and H. T. Yura, "Scintillation Effects on Centroid Anisoplanatism," *J. Opt. Soc. Am. A*, vol. 4, no. 1, p. 57, 1987.

[8] J. W. Goodman, *Statistical Optics*, Second Edi. Wiley, 1985.

[9] J. B. Burl, M. C. Roggemann, and B. Welsh, "Tilt estimation in moderate-to-strong scintillation," *Appl. Opt.*, vol. 40, no. 18, p. 2966, Jun. 2001, doi: 10.1364/AO.40.002966.

[10] M. Kalensky, M. R. Kemnetz, and M. F. Spencer, "Effects of Shock Waves on Shack–Hartmann Wavefront Sensor Data," *AIAA Journal*, vol. 61, no. 6, pp. 2356–2368, May 2023, doi: 10.2514/1.J062783.

[11] R. J. Noll, "Zernike Polynomials and Atmospheric Turbulence," *J. Opt. Soc. Am.*, vol. 66 VN-r, no. 3, p. 207, 1976.

[12] J. Ares and J. Arines, "Influence of Thresholding on Centroid Statistics: Full Analytical Description," *Appl. Opt.*, vol. 43, no. 31, pp. 5796–5805, 2004.

[13] P. Merritt and M. F. Spencer, *Beam Control for Laser System*, 2nd ed. Directed Energy Professional Society, 2018.

[14] J. W. Goodman, *Introduction to Fourier Optics*, 3rd ed. Greenwood Village, 2005.

[15] I. B. Putnam and S. C. Cain, "Modeling a Temporally Evolving Atmosphere with Zernike Polynomials," *AMOS Tech. Conf.*, 2012.

[16] J. J. Garretson, "Zernike Piston Statistics in Turbulent Multi-Aperture Optical Systems," Air Force Insitute of Technology, 2020.

[17] R. J. Sasiela, *Electromagnetic wave propagation in turbulence: evaluation and application of Mellin transforms*, 2nd ed. Bellingham, Wash: SPIE, 2007.

[18] S. Gladysz, "Absolute and Differential G-tilt in Turbulence: Theory and Applications," *Opt. Atmos. Propag. Adapt. Syst. XIX*, vol. 10002, no. November 2016, p. 100020F, 2016.

[19] G. A. Tyler, "Bandwidth considerations for tracking through turbulence," *J. Opt. Soc. Am. A*, vol. 11, no. 1, p. 358, Jan. 1994, doi: 10.1364/JOSAA.11.000358.